0888-8809/07/$15.00/0
Printed in U.S.A.

Molecular Endocrinology 21(10):2529–2540

doi: 10.1210/me.2007-0038

Pre-Spliceosomal Binding of U1 Small Nuclear Ribonucleoprotein (RNP) and Heterogenous Nuclear RNP E1 Is Associated with Suppression of a Growth Hormone Receptor Pseudoexon

Scott A. Akker, Shivani Misra, Shazad Aslam, Emma L. Morgan, Philip J. Smith, Bernard Khoo, and Shern L. Chew

Department of Endocrinology, St. Bartholomew's Hospital, London EC1A 7BE, United Kingdom

Pseudoexons occur frequently in the human genome. This paper characterizes a pseudoexon in the GH receptor gene. Inappropriate activation of this pseudoexon causes Laron syndrome. Using *in vitro* splicing assays, pseudoexon silencing was shown to require a combination of a weak 5′ pseudosplice-site and splicing silencing elements within the pseudoexon. Immunoprecipitation experiments showed that specific binding of heterogenous nuclear ribonucleoprotein E1 (hnRNP E1) and U1 small nuclear ribonucleoprotein (snRNP) in the pre-spliceosomal complex was associated with silencing of pseudoexon splicing. The possible role of hnRNP E1 was further supported by RNA interference experiments in cultured cells. Immunoprecipitation experiments with three other pseudoexons suggested that pre-spliceosomal binding of U1 snRNP is a potential general mechanism of suppression of pseudoexons. (*Molecular Endocrinology* 21: 2529–2540, 2007)

SPLICING IS THE process by which introns are precisely identified and excised with the exons ligated to form a translatable message. Alternative splicing is the process whereby alternative exons are selected from an identical pre-mRNA to give rise to two or more different mRNAs, which in turn leads to translation into different proteins. The process of alternative splicing allows a single gene to code for multiple products, thus creating an additional level of diversity and complexity.

Understanding the regulation of splicing and alternative splicing is particularly pertinent to endocrinology. Firstly, both hormones and their receptors are subject to alternative splicing which adds a further level of complexity to the endocrine regulation of gene expression, see review (1). Secondly, splicing defects are highly represented in inherited endocrine conditions, for example in congenital adrenal hyperplasia due to 21-hydroxylase deficiency (CYP21) (2, 3), multiple endocrine neoplasia type 1 (MENIN) (4), and they are the most common type of defect in neurofibromatosis type 1 (5). Thirdly, splicing defects are commonly found in all types of cancer (6–8) and, in particular, in inherited cancer syndromes (9–11).

First Published Online July 10, 2007

Abbreviations: GHR, GH receptor; hnRNP, heterogenous nuclear ribonucleoprotein; MBP, maltose binding protein; RNAi, RNA interference; siRNA, small interfering RNA; snRNP, small nuclear ribonucleoprotein.

***Molecular Endocrinology* is published monthly by The Endocrine Society (http://www.endo-society.org), the foremost professional society serving the endocrine community.**

However, although the process of splicing itself is relatively well understood (see reviews in Refs. 1, 12, and 13), the mechanisms by which the cellular machinery correctly identifies exons is not clear. It is, at least in part, dependent on loosely defined sequences termed splice sites.

Splice-site sequences that do not undergo splicing are termed pseudosites (see Ref. 14). In the human *hprt* gene, pseudosites outnumber their genuine counterparts by several hundred and, in turn, define a set of pseudoexons that outnumber the genuine exons by a factor of ten (15). It has been shown that one in three random restriction fragments of human genomic DNA contain splicing silencing properties compared with only one in 27 fragments of *E. coli* DNA (16), and computational analysis suggests that pseudoexons are associated with a 20% greater frequency of silencing elements than non-pseudoexon-containing intronic regions (17). However, the mechanism for pseudoexon skipping has only been determined for one pseudoexon in the ATM pre-mRNA, where the spliceosomal component U1 small nuclear ribonucleoprotein (U1 snRNP) was found to have a role (18). The intronic elements suppressing pseudoexon splicing have also been described for one randomly chosen pseudoexon in the human *hprt* gene (15).

The GH receptor (GHR) pseudoexon (19) is one of several pseudoexons that have been shown to cause disease when activated (Table 1). It undergoes efficient splicing when there is a single point mutation (A to G at the last nucleotide of the pseudoexon). This in turn results in the addition of 36 amino acids to the GHR leading to defective

Table 1. Genetic Diseases Caused by Pseudoexon Activation

Genetic Disease	Mutation and Location	Possible Mechanism of Activation
Cystic fibrosis (60, 61)	C to T (intron 19, CFTR), A to G (intron 11, CFTR)	Activation of 5′ pseudosites
Neurofibromatosis type II (62)	G to A (intron 5, NF2)	Creation of a branchpoint upstream of a pseudoexon
Mucopolysaccharidosis type VII (63)	TC deletion (intron 8, and β glucoronidase)	Activation of a 5′ pseudosite
Haemophilia A (64)	A to G (intron 1, factor VIII)	Activation of a 5′ pseudosite
Neurofibromatosis type I (5)	A to G (intron 30, NF1)	Activation of a 5′ pseudosite
X-linked Hypophosphataemia (30)	G to T (intron 7, PHEX)	Activation of a 5′ pseudosite
GH Insensitivity (19)	A to G (intron 6, GHR)	Activation of a 5′ pseudosite
Ataxia Telangectasia (18)	GTAA deletion (intron 20, ATM)	Loss of U1 snRNP binding site
Becker muscular dystrophy (65)	A to G (intron 62, DMD) A to G (intron 25, DMD)	Activation of a 5′ pseudosite activation of a 3′ pseudosite

Human pseudoexons have been shown to cause disease when naturally occurring mutations occur. The genetic disease caused, the nature of the mutation, and its location, together with the likely mechanism of pseudoexon activation, are shown. Only for the GHR (19) and ATM (18) pseudoexons have splicing experiments been performed to confirm that the mutation is necessary and sufficient for activation.

trafficking and the syndrome of GH insensitivity (Laron syndrome) (20). Affected patients have a variable phenotype despite harboring the same mutation (21). The point mutation changes the sequence of the pseudosplice-site from TC**A**/gtgagc (where the *slash* indicates the exon/intron boundary) to TC**G**/gtgagc. When the GHR pseudoexon is placed in a well-characterized splicing reporter (AdML-par, derived from the Adenovirus Major Late gene), it behaves in an *in vitro* splicing system as it does *in vivo* (19). To understand the mechanism of GHR pseudoexon suppression, we based experiments on *in vitro* splicing assays, immunoprecipitations, and *in vivo* splicing assays in cultured HeLa cells.

RESULTS

The Wild-Type GHR Pseudoexon 5′ Splice Site Is Not Intrinsically Defective

A bio-informatic analysis using SpliceSiteFinder (http://www.genet.sickkids.on.ca/~ali/splicesitefinder.html) was performed to assess the theoretical strengths of the pseudoexon splicing sites. This showed that the combined scores for the GHR pseudoexon branch site and splice-site scores was greater than four of the eight constitutive GHR exons, including the downstream exon 7 (Table 2). This indicated that theoretical splice-site scores alone had little predictive value for the GHR pseudoexon. However, we note that the A to G mutation leads to an increase in the 5′

Table 2. GHR Exon and Pseudoexon Splice Site Scores

GHR Exon or Pseudoexon	Length (Nucleotides)	3′ Splice Site Score	Branch Site Score	5′ Splice Site Score	3 ′, 5′, and Branch Score
1	32			**69.5**	
2	81	94.1	**81**	88.9	264
3	66	**65.6**	**89.2**	81.9	**236.7**
4	130	95.4	98.0	**65.3**	258.7
5	173	83.9	**81.0**	85.6	250.5
6	179	**74.7**	97.1	86.5	258.3
7	166	84	**83.9**	79.9	**247.8**
8	91	87.9	**62.6**	89.2	**239.7**
9	70	81.6	**71.6**	85.8	**239**
10	3425	90	**74**		
WT	108	81.6	97.1	70.3	249
MT	108	81.6	97.1	82.7	261.4

Splice-site scores for the 10 exons of the GHR and scores for wild-type (WT) and mutant (MT) pseudoexons. The table shows individual scores for the splice sites and branch point and the total combined scores. The scores that are lower than the wild-type pseudoexon are shown in *bold*. Scores for 3′ and 5′ splice sites and branch sites were calculated using Alex Dong Li's SpliceSiteFinder (http://www.genet.sickkids.on.ca/~ali/splicesitefinder.html). This algorithm for splice-site scores is based on the Shapiro and Senapathy weight matrix (66).

splice-site match to consensus, with the score increasing from 70.3 to 82.7 (Table 2).

We tested experimentally the splicing strengths of the wild-type and mutant GHR pseudoexon 5′ splice sites. It was possible that that the wild-type pseudoexon 5′ splice-site is intrinsically defective and is therefore sufficient for pseudoexon suppression. We studied the pseudoexon 5′ splice sites in isolation from the GHR pre-mRNA by using the human β-globin splicing reporter SP64-H$\beta\Delta$6-IVS1–1A (thal) (22) (Fig. 1A). The thal reporter was chosen because it is a sensitive and well-characterized 5′ splice-site reporter. A 5′ splice-site mutation in the thal exon leads to use of an upstream cryptic 5′ splice site. This gives a mRNA product of 351 nucleotides rather than the 367 nucleotide mRNA of the reporter containing the native 5′ splice site (22). We replaced the thal 5′ splice site with GHR wild-type (thal-wt) and mutant (thal-mt) 5′ splice sites (Fig. 1A) and performed *in vitro* splicing assays. Both the wild-type and mutant GHR pseudoexon splice sites underwent equivalent splicing in the thal context (Fig. 1B, lanes 7 and 10) and a comparison of the mRNA size in Fig. 1B showed an increased mRNA length in thal-wt and thal-mt compared with thal (lanes 7 and 10 *vs.* 4). These data showed that both wild-type and mutant GHR pseudoexon splice

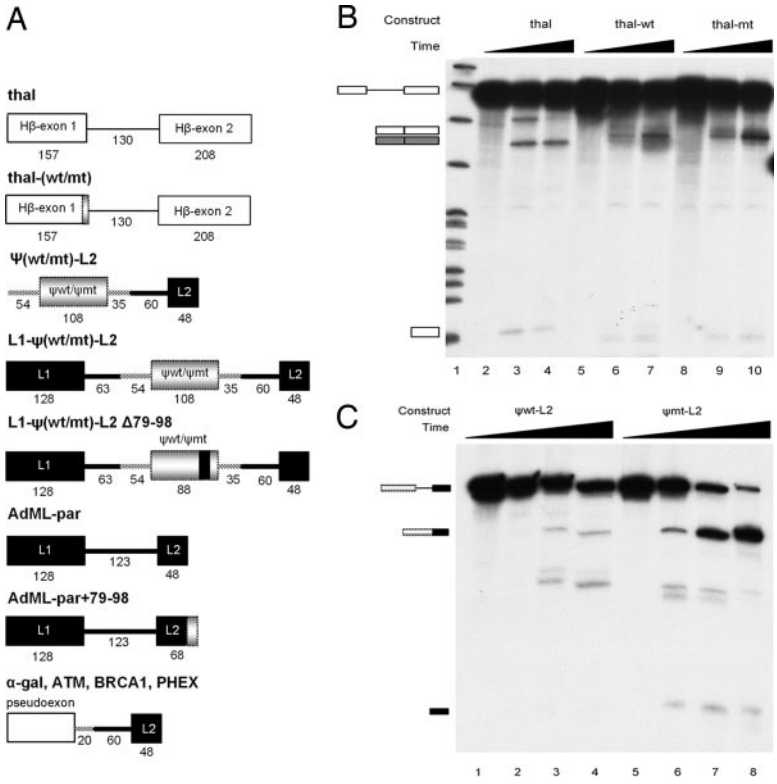

Fig. 1. The Wild-Type Pseudoexon 5′ Splice-Site Is Used Efficiently in a Different Context

A, Diagrammatic representations of the constructs used in the experiments are shown with the numbers beneath the exons (*boxes*) and introns (*lines*) representing length in nucleotides. Thal is the previously described human β-globin derived construct, SP64-H$\beta\Delta$6-IVS1–1A (22). Thal-wt and thal-mt are constructs with the thal nine-nucleotide 5′ splice site (-3 to $+6$) replaced by the GHR wild-type or mutant pseudoexon splice-site, respectively. ψwt-L2 and ψmt-L2 are constructs with the GHR pseudoexon attached to the L2 exon of AdML-par, derived from the previously described L1-ψwt-L2 and L1-ψmt-L2 constructs [AdML-ψ and AdML-ψmt in (19)]. L1-ψwt-L2Δ79–98 and L1-ψmt-L2Δ79–98 are constructs with 20 nucleotide deletions (79–98 in the example) from within the pseudoexon sequence. AdML-par is as previously described (59) and AdML-par$+$79–98 is AdML-par with the 79–98 silencer element tagged onto the 3′ end of AdML exon L2. The last diagram represents the other pseudoexon constructs with the relevant pseudoexon (α-gal, 57 nucleotides; ATM, 69 nucleotides; BRCA1, 66 nucleotides; and PHEX, 51 nucleotides) and 20 nucleotides of downstream intron attached to AdML exon L2 and its upstream intron. The final construct, Cβ, is not shown but is as previously described (25). Throughout the figures, AdML-derived exons are filled in *black*, GHR pseudoexon derived exons are *shaded gray* and *outlined with a dotted line*, and thal-derived exons are *unfilled*. B, *In vitro* splicing for the wild-type and mutant pseudoexon nine-nucleotide 5′ splice sites in the context of the thal splicing reporter. Diagrammatic representations of the pre-mRNAs and mRNAs are shown at the *side of the panel*. The mRNA with cryptic splice-site usage is *shaded gray*, and the mRNA with true splice-site usage is *unfilled*. The other splicing-dependent bands are lariat intermediates and lariat products. Lane 1 shows the standard Msp 1 digest of pBR322 run as a marker. C, *In vitro* splicing for the wild-type and mutant pseudoexon 5′ splice sites in their native contexts. These constructs are as previously described (19) without the AdML-par L1 exon and intron. As in Fig. 1B, diagrammatic representations of the pre-mRNAs and mRNAs are shown at the side of the panel. The other splicing-dependent bands are lariat intermediates and lariat products.

sites had intrinsic splicing activity and that this activity was greater than that of the reporter cryptic splice site.

Silencing Elements within the Pseudoexon Determine Skipping

We next determined the splicing effects of other sequences in the GHR pre-mRNA. We exploited *in vitro* splicing assays using chimeric pre-mRNAs. We used only the GHR pseudoexon and its splice sites in a construct containing the adenovirus major late (AdML) intron and L2 exon (ψwt-L2 and ψmt-L2 in Fig. 1A). Note that the wild-type and mutant GHR pseudoexon 5′ splice sites now lie in a limited native context, with the complete GHR pseudoexon sequence, 54 nucleotides of upstream intron and 35 nucleotides of downstream intron. There remained a significant difference ($P = 0.003$) between the splicing of the wild-type and mutant GHR pseudoexons (Fig. 1C, lanes 4 *vs.* 8), consistent with our previous data (19). This suggested that the sequences determining silencing of the GHR pseudoexon were active when the GHR pseudoexon was the leading exon and that they were confined to the GHR pseudoexon itself and/or a limited range of the surrounding introns. We also removed the GHR upstream and downstream introns and *in vitro* splicing experiments showed these had no effect on splicing (data not shown). This implied that the splicing behavior of the GHR pseudoexon is controlled via elements within the pseudoexon itself.

To systematically test for regulatory elements, a series of 20 nucleotide deletions were made along the length of both the wild-type and mutant pseudoexons (L1-ψ(wt/mt)-L2 Δ 79–98 is the example in Fig. 1A). These pseudoexons with deletions were assessed for splicing as the middle exon of the AdML-par splicing reporter (Fig. 2A). Note that the deletions were of the same length, thus acting as internal controls for nonspecific effects of GHR pseudoexon length on splicing efficiency. Inclusion of the wild-type GHR pseudoexon was seen when nucleotides 79–98 were deleted (Fig. 2A, lane 3 *vs.* lanes 1 and 9). This suggested a silencing element but one that only functioned with the wild-type GHR pseudoexon splice-site and had no silencing effect on the mutant GHR pseudoexon (compare lane 4 *vs.* lanes 2 and 10). Traces of GHR pseudoexon inclusion were seen when nucleotides 39–58 (lane 7 *vs.* 1) and nucleotides 59–78 (lane 5 *vs.* 1) were deleted. Deletion of nucleotides 3–18 had no effect on splicing (data not shown). With the 79–98 deletion there was also an increase in the wild-type pseudoexon skipped product (Fig. 2A, lane 3 *vs.* 1), suggesting that the 79–98 silencer element (when active in the wild-type context), also suppressed splicing generally between AdML-par exons L1 and L2.

The amount of wild-type GHR pseudoexon splicing was quantified. Figure 2B demonstrates that there was a 4-fold increase in the ratio of GHR pseudoexon splicing when the 79–98 element was deleted ($P = 0.005$). Figure 2C shows a diagram of the wild-type GHR pseudoexon with the 39–58 and 79–98 silencing elements and their nucleotide sequences denoted beneath. These silencing elements do not appear to resemble previously described or predicted silencing elements (17, 23, 24). Furthermore, when the GHR pseudoexon was assessed using FAS-ESS (http://genes.mit.edu/fas-ess/) (24), the only predicted splicing silencers occurred in the 19–38 region, which did

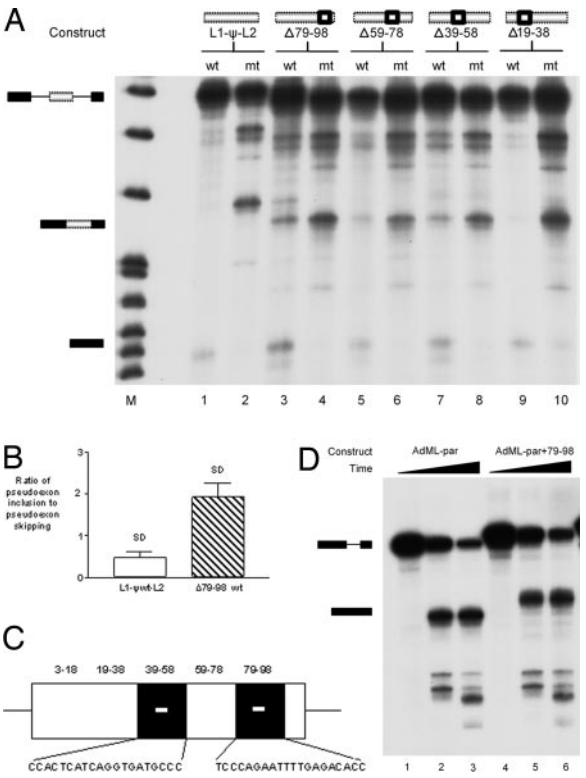

Fig. 2. Silencing Elements Occur within the Pseudoexon Sequence

A, *In vitro* splicing, at 1 h, for wild-type (wt) and mutant (mt) pseudoexons in the context of the AdML-par splicing reporter. A series of 20 nucleotide deletions were made along the length of the pseudoexons as represented by the diagrams above. The pre-mRNA, three exon mRNA, and two exon mRNA are represented by diagrams to the *left* of the panel. The pre-mRNAs and three exon mRNAs of the deletion containing pseudoexons are 20 nucleotides smaller than the full-length constructs in lanes 1 and 2. The other splicing-dependent bands are lariat intermediates and lariat products. B, The statistical analysis of the Δ79–98 deletion construct compared with full-length control from five experiments. The ratio of pseudoexon inclusion to skipping was analyzed using the NIH (Bethesda, MD) Image program for quantitative assessment. Two-tailed paired *t* test gave $P = 0.005$. C, Diagram of the pseudoexon with the principal silencing elements portrayed as *black boxes*. The 20 nucleotides that contain the silencers are shown beneath the diagram. D, *In vitro* splicing for AdML-par and AdML-par+79–98 where the 79–98 silencing element has been placed on to the 3′ end of AdML-par exon L2. Diagrammatic representations of the pre-mRNAs and mRNAs are shown at the side of the panel. The other splicing-dependent bands are lariat intermediates and lariat products.

not show silencing activity (Fig. 2A, lanes 9 and 10). The increased GHR pseudoexon splicing was not due to a nonspecific effect of decreased pseudoexon length because there was only minimal splicing with deletion of sequences 59–78 and 19–38.

Lastly, we tested whether the GHR pseudoexon 78–98 element had a general effect on silencing splicing. We positioned the element at the end of the second exon of AdML-par, a similar strategy to the characterization of the native exonic splicing silencer of the β exon of the DNA ligase III gene (25). The element did not have silencing activity when placed in this different context (Fig. 2D, compare lane 6 *vs.* 3).

Heterogenous Nuclear Ribonucleoprotein (hnRNP) E1 Interacts with the Pseudoexon and Is Important for Pseudoexon Skipping

To determine the factors acting at the GHR pseudoexon, we performed immunoprecipitation experiments with antibodies available in the lab against hnRNP A1, hnRNP E1, SF2/ASF, U1A, U1–70k and Sm. The ability of the antibodies to specifically coimmunoprecipitate radiolabeled pre-mRNAs was tested under three different *in vitro* splicing conditions; presplicing; step 1; and, splicing. Presplicing conditions were HeLa nuclear extracts held on ice, thereby allowing only the nonspecific complex H to form, but not splicing complexes E or A (13). Step 1 reactions were in HeLa nuclear extracts with ATP omitted, but incubated at 30 C, thus allowing the formation of early E and A splicing complexes, but blocking progression to later splicing steps and splicing complexes B and C. The splicing reactions were pre-mRNAs incubated at 30 C in HeLa nuclear extracts with all splicing reagents (26). Anti-maltose-binding protein (MBP) antibody was used as a control for nonspecific immunoprecipitation. hnRNP E1 specifically bound the GHR pseudoexon under presplicing conditions (Fig. 3A, lanes 7 and 8) when compared with the AdML-par control (lane 6). Furthermore, this binding was associated with GHR pseudoexon skipping because hnRNP E1 binding was 58% greater ($P = 0.015$) in the wild-type pseudoexon compared with the mutant pseudoexon (lane 7 compared with 8). Although this interaction remained detectable under step 1 conditions (lanes 13 and 14), it was lost under splicing conditions (lanes 10 and 11). The binding of hnRNP E1 with the GHR pseudoexon was detectable but was 19% ($P = 0.03$) weaker for the Δ79–98 pre-mRNAs, compared with full-length wild-type and mutant pseudoexons (Fig. 3B; lanes 11 and 12 *vs.* 9 and 10). Control immunoprecipitation experiments with the anti-MBP antibody showed no immunoprecipitation of pre-mRNA (lanes 3–5) and good recovery of appropriately spliced products, intermediates and pre-mRNA in the supernatant to show accurate loading (lanes 1 and 2). Immunoprecipitation experiments with antibodies targeting

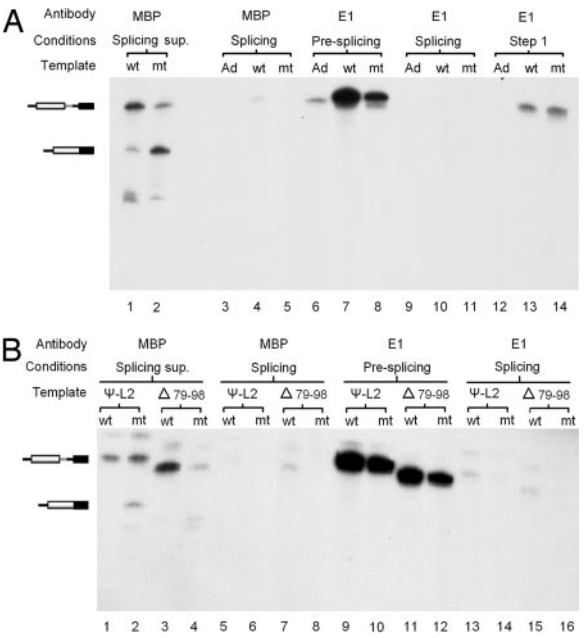

Fig. 3. The Pseudoexon Binds hnRNP E1 under Presplicing Conditions

A, Immunoprecipitations, with anti-hnRNP E1 antibody or anti-MBP antibody as a control, were performed on splicing reactions preincubated under different conditions; presplicing (4 C), Step 1 (30 C, no ATP) or splicing (30 C). The constructs used were AdML-par (Ad) as a two exon control compared with ψwt-L2 and ψmt-L2. Recovered radiolabeled pre-mRNAs were demonstrated by PAGE. Lanes 1 and 2 represent 10% of the MBP control supernatant as loading controls (less pre-mRNA correlates with more efficient splicing). Pre-mRNA and mRNA are represented by the diagrams at the side of the gel. Lanes 3–5 show background RNA recovery using the MBP control antibody with all three constructs and lanes 6, 9, and 12 represent negative controls with the AdML-par construct and hnRNP E1 antibodies. wt, Wild type; mt, mutant. B, Immunoprecipitations were repeated as above with the addition of the Δ79–98 wild-type and mutant pre-mRNAs. Lanes 1–8 are the MBP splicing supernatant loading controls and immunoprecipitation controls. Lanes 9–16 show results of immunoprecipitation with anti-hnRNP E1 antibodies for the 4 pre-mRNAs under presplicing and splicing conditions.

splicing factors hnRNP A1 and SF2/ASF did not coimmunoprecipitate pre-mRNA (data not shown).

To confirm whether hnRNP E1 was a silencer of wild-type pseudoexon splicing *in vivo*, RNA interference (RNAi) experiments were performed with small interfering RNA (siRNA) duplexes targeting the hnRNP E1 mRNA (Fig. 4). Eukaryotic expression plasmids containing the wild-type and mutant pseudoexons in the AdML-par reporter were transfected into HeLa cells and extracted RNA was assayed for splicing by RT-PCR. Panel B shows partial, but incomplete, knockdown of hnRNP E1 mRNA at 24 h (lanes 5–10) using three different targeting siRNA duplexes (H1-H3), when compared with siRNA-negative controls (lanes 1–4) and siRNA specificity controls targeting the

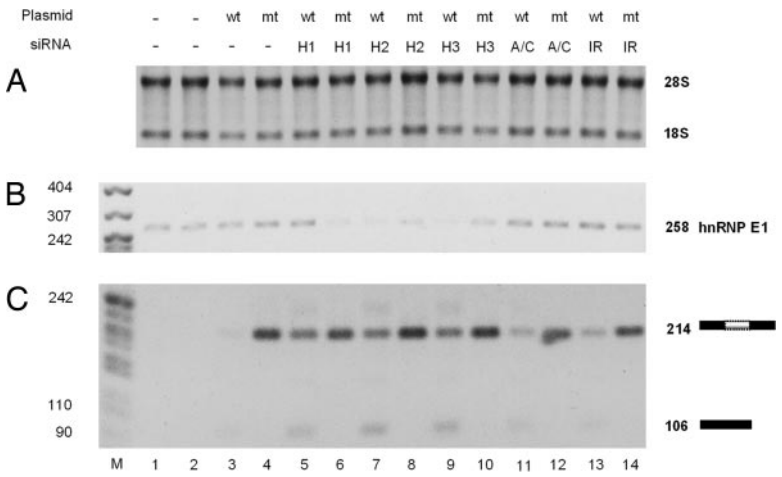

Fig. 4. hnRNP E1 Depletion Is Associated with Increased Pseudoexon Recognition

HeLa cells were transfected with pCG plasmids containing the wild-type (wt) or mutant (mt) pseudoexons within the AdML-par reporter (lanes 3–14). siRNA duplexes were cotransfected to a final concentration of 67 nmol/liter (lanes 5–14). siRNA duplexes included three siRNAs targeting three regions of the hnRNP E1 mRNA as multiplicity controls (H1, H2, and H3 in lanes 5–10). siRNAs targeting lamin A/C and insulin receptor (IR) were used as specificity controls (lanes 11–14). A, RNA loading with the principal ribosomal 28S and 18S bands labeled. The RNA was also quantified by spectrophotometry and input RNA corrected before reverse transcription. B, RT-PCR for hnRNP E1 mRNA (258 nucleotides) at 24 h after transfection. C, Splicing products for the pseudoexon plasmids with inclusion (214) or skipping (106). Lane M shows the DNA marker pBR322 Msp I. Lane 1 shows a no transfection control and lane 2 an oligofectamine alone control. Lanes 3 and 4 show plasmid transfection alone with no siRNA cotransfection.

lamin A/C and insulin receptor genes (lanes 11–14). Transfection of siRNA oligonucleotides to hnRNP E1 was associated with a 2.3-fold ($P = 0.0017$) increase in pseudoexon inclusion in the wild-type pseudoexon mini-gene (panel C, lanes 5, 7, and 9 compared with lanes 3, 11, and 13). For the statistical analysis, quantitation of pseudoexon inclusion was compared for siRNA to hnRNP E1 against the siRNA controls (lamin A/C and IR) because there was also a slight increase in splicing seen with these controls. In HeLa cells, the wild-type pseudoexon was included to a greater extent (lane 3) than the *in vitro* setting, but a splicing difference was maintained as the mutant pseudoexon was fully included (lane 4). No significant increase was seen in the mutant pseudoexon, suggesting this was not a general splicing effect. However, the splicing efficiency of the wild-type pseudoexon pre-mRNA was increased overall with siRNA against hnRNP E1 leading to an increase in both two and three exon mRNAs. This result was similar to the overall increase in splicing seen with deletion of the 79–98 silencer *in vitro* (Fig. 2A, lane 3). Protein knockdown by Western blotting was not assessed as a significant proportion of hnRNP E1 is cytoplasmic (27), and it remains possible that the antibody would cross-react with the 90% homologous protein, hnRNP E2. An additional control RT-PCR for hnRNP E2 was, however, performed and this showed no difference in hnRNP E2 mRNA levels with successful hnRNP E1 knockdown (data not shown). All of these effects were observed with a siRNA concentration of only 67 nM.

U1 snRNP Interacts with the Pseudoexon in a snRNA-Independent Way that Is Inversely Correlated to Splicing

We next investigated the interaction of U1 snRNP with pseudoexon-containing pre-mRNAs by immunoprecipitation in HeLa nuclear extracts. Immunoprecipitations were performed using antibodies against U1 snRNP core proteins: U1A and U1–70k. U1A specifically bound pseudoexon-containing pre-mRNAs under presplicing conditions (Fig. 5A, lanes 8 and 9). This contrasted with the constitutive exons of AdML-par which were only bound by U1A under splicing conditions (lanes 7 *vs.* 10). These AdML-par control data are consistent with the previously published experiments in β-globin (28).

Furthermore, as seen with hnRNP E1, the U1A binding was associated with GHR pseudoexon skipping because binding was 28% ($P = 0.03$) greater in the wild-type pseudoexon compared with the mutant pseudoexon. Preliminary experiments assessing U1A binding to pseudoexons with the 79–98 silencer removed did not show a significant reduction in U1A binding.

Under Step 1 conditions, there was also pseudoexon binding of U1A (data not shown), although this was less than under presplicing conditions as found for hnRNP E1 (Fig. 3A, lanes 13 and 14). Immunoprecipitation of the U1–70k protein gave similar results (Fig. 5B), as did immunoprecipitations with antibodies against the snRNP component Sm (data not shown). However, for U1–70k and Sm immunoprecipitations,

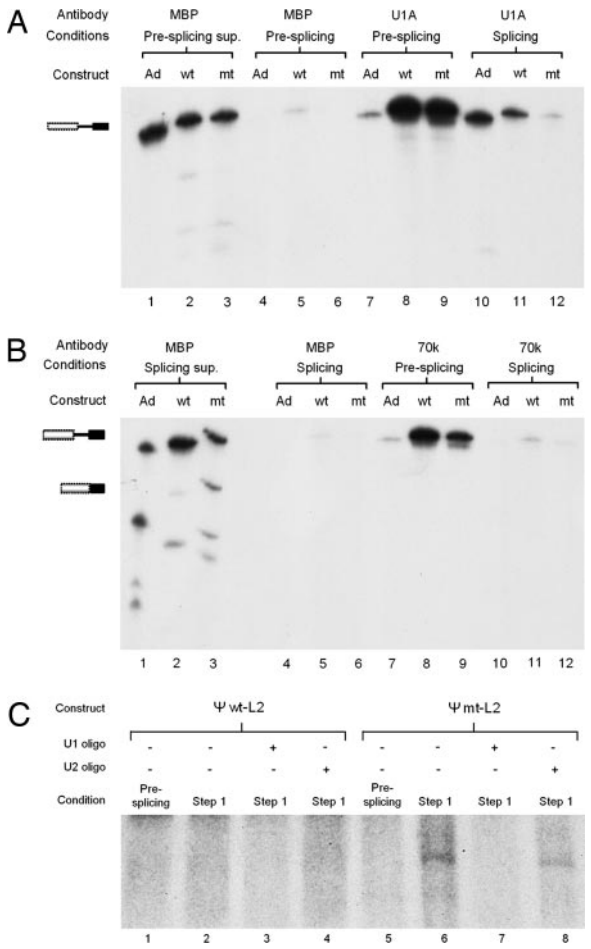

Fig. 5. Wild-Type (wt) and Mutant (mt) Pseudoexons Bind U1A under Presplicing Conditions but Only the Mutant Pseudoexon Binds U1 snRNA

A, Immunoprecipitation assays, with anti-U1A antibody were performed, as for Fig. 3, under either presplicing or splicing conditions. The constructs used were AdML-par (Ad) as a two exon control compared with ψwt-L2 and ψmt-L2. Lanes 1–3 represent 10% MBP loading controls. The MBP controls were performed under presplicing conditions. Lanes 4–6 show RNA recovery with anti-MBP antibodies and lanes 7–12 show results for anti-U1A antibody under presplicing and splicing conditions. B, Immunoprecipitation assays, with anti-U1 70k antibody were performed, as for Fig. 5C, except that the MBP controls in this experiment were performed under splicing conditions. The diagrams to the *left* represent the pre-mRNA and mRNA products of the splicing supernatant. C, Pre-mRNA/snRNA UV cross-linking was performed under step 1 conditions. Wild-type (lanes 1–4) and mutant (lanes 5–8) pseudoexon-containing pre-mRNAs (ψwt-L2 and ψmt-L2) were incubated in a step 1 splicing assay (30 C, without ATP) except lanes 1 and 5 that were incubated under presplicing conditions (4 C). Nuclear extracts in lanes 3 and 7 were preincubated with oligonucleotides targeting the U1 snRNA as a U1 snRNA specificity control and extracts in lanes 4 and 8 were preincubated with oligonucleotides targeting the U2 snRNA.

AdML-par was not immunoprecipitated under splicing conditions, suggesting that the antibody binding site is inaccessible. The U1–70k and Sm antibodies have principally been used for snRNP immunoprecipitation rather than snRNP/pre-mRNA coimmunoprecipitation.

UV cross-linking studies (Fig. 5C) showed that U1 snRNA only cross-linked to the mutant pseudoexon (lane 6 *vs.* 2) ($P = 0.028$) under splicing conditions (lane 6 *vs.* 5). No cross-linking was seen under presplicing conditions and depletion of U1 snRNA resulted in loss of cross-linking to the mutant pseudoexon (lane 7 *vs.* 6).

U1 snRNP Undergoes a Pre-Spliceosomal Interaction with Other Pseudoexons

To test whether pre-spliceosomal binding of U1 snRNP occurs in other pseudoexons and alternative exons, immunoprecipitation experiments were performed in extracts mixed with pre-mRNAs on ice. The immunoprecipitating antibody was to U1A as in Fig. 5A. The test pre-mRNAs were: two rarely used alternative exons derived from the α galactosidase (29) and DNA ligase III (25) genes; and, three other pseudoexons with naturally occurring disease causing mutations derived from the ATM (18), PHEX (30), and BRCA1 (31) genes. AdML-par pre-mRNA was used as a negative control because this contains a constitutive intron efficiently interacting with U1 snRNP only under full splicing conditions (Fig. 5A, lane 10) but weakly under pre-spliceosomal conditions (Fig. 5A, lane 7). Bacterial kanamycin resistance mRNA was used as an intronless negative control RNA to show nonspecific binding. Figure 6A shows that all the exons and pseudoexons tested had increased binding of U1A compared with AdML-par pre-mRNA and bacterial kanamycin resistance mRNA controls. In two of the three examples (GHR and ATM) where the naturally occurring mutations were compared with the native exon, U1A binding was reduced in the splicing active context (lanes 5 *vs.* 4 and 9 *vs.* 8).

DISCUSSION

Numerous pseudosites within introns are actively suppressed (15–18). The GHR pseudoexon has provided a model with which to explore pseudoexon suppression. Our analysis indicated poor pseudosite and pseudoexon prediction by bio-informatic criteria. The finding that the wild-type GHR pseudoexon 5′ splice-site was capable of efficient splicing when placed in a constitutive exon suggested the repressive influence of other sequences in the pseudoexon. The deletion experiments showed that the wild-type 5′ splice-site suppression is, in part, due to the presence of silencing elements within the pseudoexon. Silencing elements in proximity to the pseudoexon have been described for both the *hprt* (15) and ATM (18) pseudoexons, but the GHR pseudoexon Δ79–98 element was surprising in that it appeared to only have an effect on wild-type but not mutant pseudoexon splic-

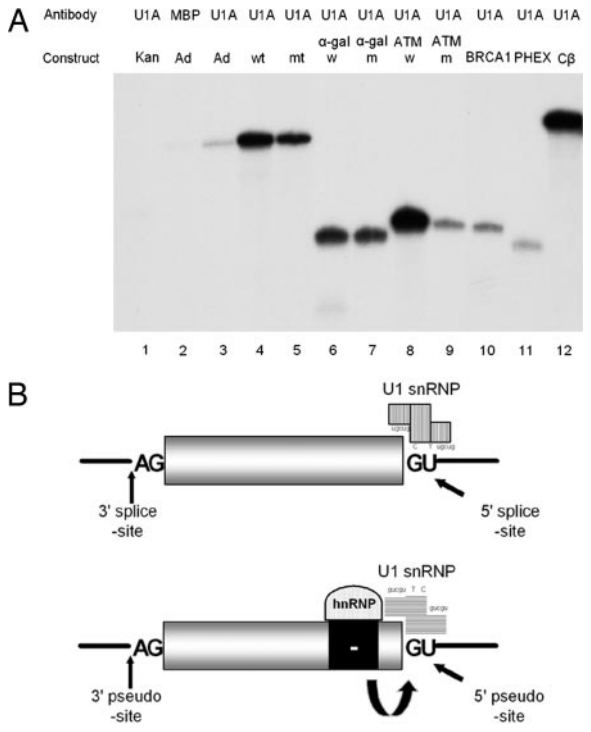

Fig. 6. U1 Interacts with Other Pseudoexons and Alternative Exons under Presplicing Conditions

A, Immunoprecipitation assays, with anti-U1A antibody, were performed against a panel of different pre-mRNAs under presplicing conditions. Negative control constructs included the bacterial kanamycin resistance gene (Kan) in lane 1 and AdML-par (Ad) in lane 3. Wild-type and mutated pre-mRNAs are shown for the first three exons, the GHR pseudoexon [wild-type (wt) and mutant (mt)], the α-galactosidase alternative exon (α-gal w and m) and the Ataxia Telangectasia pseudoexon (ATM w and m). Wild-type pre-mRNAs only are shown for the BRCA1 pseudoexon, the PHEX pseudoexon and the DNA ligase III alternative exon (Cβ). B, The *upper diagram* represents the U1 snRNP interaction with a true 5′ splice-site. The U1 snRNA is represented by the letters between the U1 snRNP and the 5′ splice-site. The *lower diagram* shows a model of pseudoexon repression where a hnRNP interacts with a silencing element and U1 snRNP to identify the 5′ pseudo-site. A different conformation of U1 snRNP is represented by the changed shading and diversion of the snRNA from the 5′ splice-site. The U1 snRNA does not base-pair with the pseudo-site and spliceosome formation is blocked. This hnRNP/U1 snRNP/pre-mRNA interaction occurs early, before possible spliceosome formation. A, Adenine; G, guanine; U, uracil.

ing. We acknowledge that deletion mutants may create new hybrid sequences that might influence splicing. However, the specific effect of the GHR pseudoexon Δ79–98 on the splicing of the wild-type pseudoexon but not on the mutant suggests a new hybrid enhancer interaction is unlikely.

hnRNP E1 interacted with the GHR pseudoexon under presplicing conditions in a manner that is inversely related both to splicing itself and splicing conditions. Thus, the interaction was greater in the wild type than in the mutant, and the protein bound to the pre-mRNA only significantly on ice, with the immunoprecipitation diminishing as the conditions are brought closer to splicing ones (first in an extract halted at step 1, then a full splicing extract). The loss of detectable hnRNP E1 under splicing conditions would be compatible with the known role of SR proteins and hnRNPs in recruiting additional factors (see review in Ref. 14). For example, one speculation is that recruitment of additional factors rapidly occurs, thereby displacing hnRNP E1. The RNAi results support a role for hnRNP E1 in silencing of the GHR pseudoexon. Knockdown of hnRNP E1 leads to an increase in splicing of wild-type pseudoexon-containing pre-mRNAs with no increase seen in mutant pseudoexon-containing pre-mRNAs. If the knockdown of hnRNP E1 led to a nonspecific increase in splicing, one would predict an increase in the mutant pseudoexon-containing mRNA also. We acknowledge that RNAi of hnRNP E1 *in vivo* showed a wider increase in splicing activity than the *in vitro* experiments, which may reflect undefined differences in the RNA reporters or cell constituents. Furthermore, we acknowledge that there are considerable technical difficulties in RNAi of hnRNP E1 and hnRNP proteins in general. The difficulties reflect their nuclear abundance, the lack of complete knockdown by siRNA and their binding to multiple sites, as typified by hnRNP A1 (32). hnRNP E1 transfection post-siRNA and experiments with 79–98 silencer-deleted pseudoexons could provide more powerful evidence of hnRNP E1 involvement, but we believe the current data do partly support the *in vitro* data. hnRNP E1 (also termed PCBP 1 and αCP 1) has roles in translation and mRNA stability and is found in both the nucleus and cytoplasm (see Ref. 27 for review). It does, however, colocalize in nuclear speckles with the splicing factor SC35, suggesting a possible role in splicing (33).

The U1A immunoprecipitation data suggested that U1 snRNP was also interacting with both wild-type and mutant pseudoexons before expected spliceosome formation and, as with hnRNP E1, the interaction was inversely correlated to splicing conditions. However, the interaction of U1 snRNP with the wild-type pseudoexon was biochemically distinct from the characteristics of its interaction with true exons. For true exons (for example AdML-par, in Fig. 5A), U1 snRNP bound the 5′ splice-site in splicing extracts at 30 C, before the need for ATP, but not while the *in vitro* reactions were on ice (28). This unexpected pre-spliceosomal interaction occurred in the five other pseudoexons or rarely used alternative exons that were tested. As with hnRNP E1, the U1 snRNP interaction was not detectable in the pseudoexons under splicing conditions and we hypothesize that this is due to either, displacement of the U1 snRNP by another complex or recruitment of other factors around the U1 snRNP.

The U1 snRNA/5′ splice-site interaction is an important part of accurate and specific splicing (34). Splicing is significantly reduced with U1 snRNA depletion, but

U1 snRNP is still capable of interacting with 5′ splice sites both in yeast (35) and in mammals (34, 36). That U1 snRNP may act as a suppressor of pseudoexon splicing is plausible because it is recognized that U1 snRNP can act in an inhibitory manner. In mammals, proximity of 5′ consensus splice sites inhibits splicing (28, 37, 38), and there are several models in which U1 snRNP is proposed to have an inhibitory role. Exonic splicing enhancers are known to encourage U1 snRNP binding to genuine 5′ splice sites (28, 39) but work on the *Drosophila* P-element shows that, in a contrasting manner, U1 snRNP may bind pseudosites, together with silencers, to actually disrupt splicing at the genuine 5′ splice-site. This allows regulation of alternative splicing of the P-element third intron (40). Similar work demonstrates that U1 snRNP also has a role in the skipping of a pseudoexon within intron 20 of the ATM gene (18). Finally, a U1 snRNP complex has been shown to bind 5′ pseudosites within viral negative regulatory elements of the Rous sarcoma virus (41) and the human papilloma virus type 16 (42). Interestingly hnRNP E1 has been shown to also bind the same region of the human papilloma virus 16 mRNA (43).

The data above would support the previously described models of 5′ splice-site selection (44, 45) to include pseudosites. Thus, for 5′ pseudosites, inhibitory splicing factors act to destabilize the potential U1 snRNA/5′ splice-site interaction. Early, pre-spliceosomal binding (complex H) of the silencers and U1 snRNP would ensure that these sites are safely isolated. U1 snRNP binding may be in a different configuration. The cross-linking data (Fig. 5C) could be explained if this were the case. Cross-linking of the U1 snRNA to the pre-mRNA was only seen in the mutant under STEP 1 conditions, as would be predicted if the U1 snRNA/pre-mRNA interaction is a prerequisite to splicing. The presplicing U1A immunoprecipitations (Fig. 5A) suggest that there was a U1 snRNP/pre-mRNA interaction, but the lack of cross-linking in both wild-type and mutant pre-mRNAs under presplicing conditions suggested that this interaction is indeed different.

Figure 6B is a diagrammatic model of this potential U1 snRNP interaction. The upper diagram shows the U1 snRNP interacting with an active 5′ splice site (such as the mutant pseudoexon). The U1 snRNA base pairs with the 5′ splice site and recruits the spliceosome. The lower diagram shows the pseudoexon silencer interacting with the 5′ splice site. The interaction leads to the early recruitment of a hnRNP and U1 snRNP. However, the U1 snRNP does not interact in an active conformation, and thus blocks further recruitment of spliceosomal factors. By temporally ensuring that this inhibitory U1 snRNP role occurs before active U1 snRNP interactions, splicing fidelity is maintained. The model is likely to be an over simplification because our data suggest the presence of more than one silencing element (Fig. 3A) and more than one hnRNP E1 binding site (Fig. 4B). One possibility is that cooperative binding of other silencing factors would follow an initial interaction. This model would be the mammalian equivalent of that proposed for the *Drosophila* P-element, which also does not require base pairing between the U1 snRNA and target pre-mRNA (40). There is some further published evidence to support such a role for hnRNPs and U1 snRNP: 1) It has previously been demonstrated that hnRNP A1 leads to decreased U1 snRNA/pre-mRNA base pairing (46–48); 2) Several systematically identified exonic splicing silencers are also 5′ pseudosites (24); and 3) U1 snRNP is the most abundant snRNP, with twice the number of copies per cell when compared with U2 snRNP and five times the copies of U4 and U5 snRNPs (49). These data suggest a potential additional role of a U1 snRNP/hnRNP interaction to identify and isolate potential 5′ splice sites. Our data also suggest that a defect in the mechanism of suppression of pseudoexon splicing could result in GHR pseudoexon inclusion and Laron syndrome. There may well be other similar examples of intronic mutations leading to removal of pseudoexon suppression, and resulting in genetic disease.

MATERIALS AND METHODS

Construction of Pre-mRNA Templates

Templates were made as described (19) by overlap extension PCR. Oligonucleotide sequences are available on request. Radiolabeled pre-mRNAs were transcribed with SP6 or T7 RNA polymerase using [α-^{32}P-GTP] and then gel purified.

Splicing Reactions

The 25-μl splicing reactions were performed using 20 fmol of pre-mRNA, incubated with HeLa cell nuclear extract splicing mix as described (50), under presplicing (0 C), Step 1 (30 C but without ATP) or splicing (30 C) conditions.

Immunoprecipitations

Anti-MBP antibodies (51) and anti-U1 70k (2.73) antibodies (52) were kindly provided by Adrian Krainer (Cold Spring Harbor Laboratory, Cold Spring Harbor, NY). Anti-U1A (1E1) antibodies (53) were kindly provided by J. Alwine (University of Pennsylvania, Philadelphia, PA) and anti-hnRNP E1 (GSTE1) antibodies (54) by Asok Antony (Indiana University, Indianapolis, IN). Experiments were essentially performed as described (50). Briefly, Protein G Sepharose beads (Amersham Biosciences, Buckinghamshire, UK) were washed and incubated overnight at 4 C with antimouse or, for GSTE1, antirabbit IgG. After three further washes in buffer IP150, the specific antibodies were then prebound for 2 h at 4 C. After three further washes, 25-μl splice reactions with 475 μl IP150 buffer were added and incubated for 1 h at 4 C. The final three washes were performed with IP150 buffer containing 0.5 mg/ml tRNA. The resuspended pellet underwent phenol extraction and ethanol precipitation.

RNAi Cotransfections

Three siRNAs targeting hnRNP E1 mRNA were selected using recognized criteria (55) from a list generated by the Dharmacon on-line siRNA design center, after a BLAST search

(H1; AAGAGATCCGCGAGAGTAC, H2; CTCGATTCAAGGACAACAC, H3; CTTAATTGGCTGCATAATC). siRNAs targeting the insulin receptor and Lamin A/C mRNA were ordered as specificity controls. Mini-gene systems expressing wild-type or mutant pseudoexons were made by subcloning the described AdML-par pseudoexon constructs (19) into pCG plasmids. HeLa cells were seeded in 24-well plates at a concentration of 100,000/ml in a final volume of 0.5 ml. Cells were treated at 24 h with siRNA, using transfection protocols previously described (56, 57), with the following changes: siRNA was added to a final concentration of 67 nM and was cotransfected with 1 μg of the wild-type or mutant pseudoexon mini-gene. Previous titration experiments had established the minimum effective dose to knock down hnRNP E1 expression with minimal cell toxicity.

RNA was harvested from cells 24 h after transfection using the QIAGEN (Sussex, UK) RNeasy kit as per the manufacturer's instructions. The RNA was subjected to an additional deoxyribonuclease digestion step using ribonuclease-free RQ1DNase enzyme (Promega, Southampton, UK). RT-PCR was performed, with equal RNA loading (400 ng/reaction) ensured by standardization of concentrations using spectrophotometric readings. cDNA was subjected to PCR assaying for hnRNP E1 mRNA, hnRNP E2 mRNA and GHR pseudoexon splicing products.

UV Cross-Linking Studies

Step 1 splicing reactions were preincubated, for 15 min at 30 C, with 1 μl oligonucleotide (400 μM) complementary to the U1 or U2 snRNA as previously described (58), before adding 20 fmol RNA. Ten microliters of each 25-μl reaction were then added to 0.4 μl of ATP/CP and standard splicing control reactions were performed to ensure satisfactory U1/U2 depletion (data not shown). The remaining 15-μl reactions were incubated at 30 C for 30 min and then, on ice, exposed to 9000J $\times$ 2 of UV light. Fifty microliters of Proteinase K mix were added and each reaction incubated for 15 min at 37 C. Samples were then phenol extracted, ethanol precipitated and visualized by PAGE.

Statistical Analyses

High resolution scans of the SDS-PAGE gels were quantified using Fujifilm (Tokyo, Japan) Multigauge version 2.3 software. GraphPad (San Diego, CA) prism software was used to analyze the data and the *P* values stated are the results of two-tailed *t* tests.

Acknowledgments

We are very grateful to A. Krainer (Cold Spring Harbor Laboratory, Cold Spring Harbor, NY), J. Alwine (University of Pennsylvania, Philadelphia PA), and A. Antony (Indiana University, Indianapolis, IN) for their generous gifts of antibodies. We are grateful to G. Makarov, O. Makarova, and I. Eperon (all from the University of Leicester, Leicestershire, UK) for helpful discussion.

Received January 22, 2007. Accepted July 6, 2007.

Address all correspondence and requests for reprints to: Dr. Scott A. Akker, Department of Endocrinology, 5th Floor, King George V Block, St Bartholomew's Hospital, West Smithfield, London EC1A 7BE, United Kingdom. E-mail: s.a.akker@qmul.ac.uk.

S.A. was supported by a Wellcome Training Fellowship from The Wellcome Trust (GR067291MA).

Disclosure Statement: None of the authors have any potential conflict to declare.

REFERENCES

1. Akker SA, Smith PJ, Chew SL 2001 Nuclear post-transcriptional control of gene expression. J Mol Endocrinol 27:123–131
2. Long M, de Souza S, Rosenberg C, Gilbert W 1998 Relationship between "proto-splice sites" and intron phases: evidence from dicodon analysis. Proc Natl Acad Sci USA 95:219–223
3. Kapelari K, Ghanaati Z, Wollmann H, Ventz M, Ranke MB, Kofler R, Peters H 1999 A rapid screening for steroid 21-hydroxylase mutations in patients with congenital adrenal hyperplasia. Mutations in brief no. 247. Online. Hum Mutat 13:505
4. Mutch MG, Dilley WG, Sanjurjo F, DeBenedetti MK, Doherty GM, Wells SAJ, Goodfellow PJ, Lairmore TC 1999 Germline mutations in the multiple endocrine neoplasia type 1 gene: evidence for frequent splicing defects. Hum Mutat 13:175–185
5. Ars E, Serra E, Garcia J, Kruyer H, Gaona A, Lazaro C, Estivill X 2000 Mutations affecting mRNA splicing are the most common molecular defects in patients with neurofibromatosis type 1. Hum Mol Genet 9:237–247
6. Kalnina Z, Zayakin P, Silina K, Line A 2005 Alterations of pre-mRNA splicing in cancer. Genes Chromosomes Cancer 42:342–357
7. Kaufmann D, Leistner W, Kruse P, Kenner O, Hoffmeyer S, Hein C, Vogel W, Messiaen L, Bartelt B 2002 Aberrant splicing in several human tumors in the tumor suppressor genes neurofibromatosis type 1, neurofibromatosis type 2, and tuberous sclerosis 2. Cancer Res 62:1503–1509
8. Driouch K, Prydz H, Monese R, Johansen H, Lidereau R, Frengen E 2002 Alternative transcripts of the candidate tumor suppressor gene, WWOX, are expressed at high levels in human breast tumors. Oncogene 21:1832–1840
9. Claes K, Vandesompele J, Poppe B, Dahan K, Coene I, De Paepe A, Messiaen L 2002 Pathological splice mutations outside the invariant AG/GT splice sites of BRCA1 exon 5 increase alternative transcript levels in the 5′ end of the BRCA1 gene. Oncogene 21:4171–4175
10. Lefevre SH, Chauveinc L, Stoppa-Lyonnet D, Michon J, Lumbroso L, Berthet P, Frappaz D, Dutrillaux B, Chevillard S, Malfoy B 2002 A T to C mutation in the polypyrimidine tract of the exon 9 splicing site of the RB1 gene responsible for low penetrance hereditary retinoblastoma. J Med Genet 39:E21
11. Gavert N, Yaron Y, Naiman T, Bercovich D, Rozen P, Shomrat R, Legum C, Orr-Urtreger 2002 A molecular analysis of the APC gene in 71 Israeli families: 17 novel mutations. Hum Mutat 19:664
12. Staley JP, Guthrie C 1998 Mechanical devices of the spliceosome: motors, clocks, springs, and things. Cell 92:315–326
13. Reed R, Oalandjian L 2000 Spliceosome assembly. In: Krainer AR, ed. Eukaryotic mRNA processing. Oxford, UK: IRL Press; 103–129
14. Cartegni L, Chew SL, Krainer AR 2002 Listening to silence and understanding nonsense: exonic mutations that affect splicing. Nat Rev Genet 3:285–298
15. Sun H, Chasin LA 2000 Multiple splicing defects in an intronic false exon. Mol Cell Biol 20:6414–6425
16. Fairbrother WG, Chasin LA 2001 Human genomic sequences that inhibit splicing. Mol Cell Biol 20:6816–6825
17. Zhang XH, Chasin LA 2004 Computational definition of sequence motifs governing constitutive exon splicing. Genes Dev 18:1241–1250
18. Pagani F, Buratti E, Stuani C, Bendix R, Dork T, Baralle FE 2002 A new type of mutation causes a splicing defect in ATM. Nat Genet 30:426–429
19. Metherell LA, Akker SA, Munroe PB, Rose SJ, Caulfield M, Savage MO, Chew SL, Clark AJ 2001 Pseudoexon activation as a novel mechanism for disease resulting in

atypical growth-hormone insensitivity. Am J Hum Genet 69:641–646
20. Maamra M, Milward A, Esfahani HZ, Abbott LP, Metherell LA, Savage MO, Clark AJ, Ross RJ 2006 A 36 residues insertion in the dimerization domain of the growth hormone receptor results in defective trafficking rather than impaired signaling. J Endocrinol 188:251–261
21. David A, Camacho-Hubner C, Bhangoo A, Rose SJ, Miraki-Moud F, Akker SA, Butler GE, Ten S, Clayton PE, Clark AJ, Savage MO, Metherell LA 2007 An intronic growth hormone receptor mutation causing activation of a pseudoexon is associated with a broad spectrum of growth hormone insensitivity phenotypes. J Clin Endocrinol Metab 92:655–659
22. Krainer AR, Maniatis T, Ruskin B, Green MR 1984 Normal and mutant human β-globulin pre-mRNAs are faithfully and efficiently spliced in vitro. Cell 36:993–1005
23. Pozzoli U, Riva L, Menozzi G, Cagliani R, Comi GP, Bresolin N, Giorda R, Sironi M 2004 Over-representation of exonic splicing enhancers in human intronless genes suggests multiple functions in mRNA processing. Biochem Biophys Res Commun 322:470–476
24. Wang Z, Rolish ME, Yeo G, Tung V, Mawson M, Burge CB 2004 Systematic identification and analysis of exonic splicing silencers. Cell 119:831–845
25. Chew SL, Baginsky L, Eperon IC 2000 An exonic splicing silencer in the testes-specific DNA ligase III β exon. Nucleic Acids Res 28:402–410
26. Mayeda A, Krainer AR 1998 Preparation of Hela cell nuclear and cytosolic S100 extracts for in vitro splicing. In: Haynes SR, ed. RNA-protein interaction protocols. Totowa, NJ: Humana Press
27. Makeyev AV, Liebhaber SA 2002 The poly(C)-binding proteins: a multiplicity of functions and a search for mechanisms. RNA 8:265–278
28. Eperon IC, Ireland DC, Smith RA, Mayeda A, Krainer AR 1993 Pathways for selection of the 5′ splice sites by U1 snRNPs and SF2/ASF. EMBO J 12:3607–3617
29. Ishii S, Nakao S, Minamikawa-Tachino R, Desnick RJ, Fan JQ 2002 Alternative splicing in the α-galactosidase A gene: increased exon inclusion results in the Fabry cardiac phenotype. Am J Hum Genet 70:994–1002
30. Christie PT, Harding B, Nesbit MA, Whyte MP, Thakker RV 2001 X-linked hypophosphatemia attributable to pseudoexons of the PHEX gene. J Clin Endocrinol Metab 86:3840–3844
31. Balz V, Prisack HB, Bier H, Bojar H 2002 Analysis of BRCA1, TP53, and TSG101 germline mutations in German breast and/or ovarian cancer families. Cancer Genet Cytogenet 138:120–127
32. Patry C, Bouchard L, Labrecque P, Gendron D, Lemieux B, Toutant J, Lapointe E, Wellinger R, Chabot B 2003 Small interfering RNA-mediated reduction in heterogeneous nuclear ribonucleoparticule A1/A2 proteins induces apoptosis in human cancer cells but not in normal mortal cell lines. Cancer Res 63:7679–7688
33. Chkheidze AN, Liebhaber SA 2003 A novel set of nuclear localization signals determine distributions of the αCP RNA-binding proteins. Mol Cell Biol 23:8405–8415
34. Tarn WY, Steitz JA 1994 SR proteins can compensate for the loss of U1 snRNP functions in vitro. Genes Dev 8:2704–2717
35. Du H, Rosbash M 2001 Yeast U1 snRNP-pre-mRNA complex formation without U1snRNA-pre-mRNA base pairing. RNA 7:133–142
36. Lund M, Kjems J 2002 Defining a 5′ splice site by functional selection in the presence and absence of U1 snRNA 5′ end. RNA 8:166–179
37. Carothers AM, Urlaub G, Grunberger D, Chasin LA 1993 Splicing mutants and their second-site suppressors at the dihydrofolate reductase locus in Chinese hamster ovary cells. Mol Cell Biol 13:5085–5098
38. Cooke C, Hans H, Alwine JC 1999 Utilization of splicing elements and polyadenylation signal elements in the coupling of polyadenylation and last-intron removal. Mol Cell Biol 19:4971–4979
39. Kohtz JD, Jamison SF, Will CL, Zuo P, Luhrmann R, Garcia-Blanco MA, Manley JL 1994 Protein-protein interactions and 5′-splice-site recognition in mammalian mRNA precursors. Nature 368:119–124
40. Labourier E, Adams MD, Rio DC 2001 Modulation of P-element pre-mRNA splicing by a direct interaction between PSI and U1 snRNP 70K protein. Mol Cell 8:363–373
41. McNally LM, McNally MT 1999 U1 small nuclear ribonucleoprotein and splicing inhibition by the Rous sarcoma virus negative regulator of splicing element. J Virol 73: 2385–2393
42. Cumming SA, McPhillips MG, Veerapraditsin T, Milligan SG, Graham SV 2003 Activity of the human papillomavirus type 16 late negative regulatory element is partly due to four weak consensus 5′ splice sites that bind a U1 snRNP-like complex. J Virol 77:5167–5177
43. Collier B, Goobar-Larsson L, Sokolowski M, Schwartz S 1998 Translational inhibition in vitro of human papillomavirus type 16 L2 mRNA mediated through interaction with heterogenous ribonucleoprotein K and poly(rC)-binding proteins 1 and 2. J Biol Chem 273:22648–22656
44. Eperon LC, Estibeiro JP, Eperon IC 1986 The role of nucleotide sequences in splice selection in eukaryotic pre-messenger RNA. Nature 324:280–282
45. Roca X, Sachidanandam R, Krainer AR 2005 Determinants of the inherent strength of human 5′ splice sites. RNA 11:683–698
46. Chabot B, Blanchette M, Lapierre I, La Branche H 1997 An intron element modulating 5′ splice site selection in the hnRNP A1 pre-mRNA interacts with hnRNP A1. Mol Cell Biol 17:1776–1786
47. Nasim FU, Hutchison S, Cordeau M, Chabot B 2002 High-affinity hnRNP A1 binding sites and duplex-forming inverted repeats have similar effects on 5′ splice site selection in support of a common looping out and repression mechanism. RNA 8:1078–1089
48. Eperon IC, Makarova OV, Mayeda A, Munroe SH, Caceres JF, Hayward DG, Krainer AR 2000 Selection of alternative 5′ splice sites: role of U1 snRNP and models for the antagonistic effects of SF2/ASF and hnRNP A1. Mol Cell Biol 20:8303–8318
49. Baserga SJ, Steitz JA 1993 The diverse world of small ribonucleoproteins. In: Gesteland RF, Atkins JF, eds. The RNA world. Cold Spring Harbor, NY: Cold Spring Harbor Laboratory Press; 359–381
50. Smith PJ, Spurrell EL, Coakley J, Hinds CJ, Ross RJ, Krainer AR, Chew SL 2002 An exonic splicing enhancer in human IGF-I pre-mRNA mediates recognition of alternative exon 5 by the serine-arginine protein splicing factor-2/ alternative splicing factor. Endocrinology 143: 146–154
51. Hanamura A, Caceres JF, Mayeda A, Franza Jr BR, Krainer AR 1998 Regulated tissue-specific expression of antagonistic pre-mRNA splicing factors. RNA 4:430–444
52. Takeda Y, Nyman U, Winkler A, Wise KS, Hoch SO, Pettersson I, Anderson SK, Wang RJ, Wang GS, Sharp GC 1991 Antigenic domains on the U1 small nuclear ribonucleoprotein-associated 70K polypeptide: a comparison of regions selectively recognized by human and mouse autoantibodies and by monoclonal antibodies. Clin Immunol Immunopathol 61:55–68
53. O'Connor JP, Alwine JC, Lutz CS 1997 Identification of a novel, non-snRNP protein complex containing U1A protein. RNA 3:1444–1455
54. Xiao X, Tang YS, Mackins JY, Sun XL, Jayaram HN, Hansen DK, Antony AC 2001 Isolation and characterization of a folate receptor mRNA-binding trans-factor from human placenta. Evidence favoring identity with hetero-

geneous nuclear ribonucleoprotein E1. J Biol Chem 276: 41510–41517
55. Dykxhoorn DM, Novina CD, Sharp PA 2003 Killing the messenger: short RNAs that silence gene expression. Nat Rev Mol Cell Biol 4:457–467
56. Elbashir SM, Harborth J, Lendeckel W, Yalcin A, Weber K, Tuschl T 2001 Duplexes of 21-nucleotide RNAs mediate RNA interference in cultured mammalian cells. Nature 411:494–498
57. Elbashir SM, Lendeckel W, Tuschl T 2001 RNA interference is mediated by 21- and 22-nucleotide RNAs. Genes Dev 15:188–200
58. Krainer A, Maniatis T 1985 Multiple factors including the small nuclear ribonucleoproteins U1 and U2 are necessary for pre-mRNA splicing in vitro. Cell 42:725–736
59. Anderson K, Moore MJ 1997 Bimolecular exon ligation by the human spliceosome. Science 276:1712–1716
60. Highsmith WE, Burch LH, Zhou Z, Olsen JC, Boat TE, Spock A, Gorvoy JD, Quittel L, Friedman KJ, Silverman LM 1994 A novel mutation in the cystic fibrosis gene in patients with pulmonary disease but normal sweat chloride concentrations. N Engl J Med 331:974–980
61. Chillon M, Dork T, Casals T, Gimenez J, Fonknechten N, Will K, Ramos D, Nunes V, Estivill X 1995 A novel donor splice site in intron 11 of the CFTR gene, created by mutation 1811+1.6kbA->G, produces a new exon: high frequency in Spanish cystic fibrosis chromosomes and association with severe phenotype. Am J Hum Genet 56:623–629
62. De Klein A, Riegman PH, Bijlsma EK, Heldoorn A, Muijtjens M, den Bakker MA, Avezaat CJ, Zwarthoff EC 1998 A G–>A transition creates a branch point sequence and activation of a cryptic exon, resulting in the hereditary disorder neurofibromatosis 2. Hum Mol Genet 7:393–398
63. Vervoort R, Gitzelmann R, Lissens W, Liebaers I 1998 A mutation (IVS8+0.6kbdelTC) creating a new donor splice site activates a cryptic exon in an Alu-element in intron 8 of the human β-glucuronidase gene. Hum Genet 103: 686–693
64. Bagnall RD, Waseem NH, Green PM, Colvin B, Lee C, Giannelli F 1999 Creation of a novel donor splice site in intron 1 of the factor VIII gene leads to activation of a 191 bp cryptic exon in two haemophilia A patients. Br J Haematol 107:766–771
65. Tuffery-Giraud S, Saquet C, Chambert S, Claustres M 2003 Pseudoexon activation in the DMD gene as a novel mechanism for Becker muscular dystrophy. Hum Mutat 21:608–614
66. Shapiro MB, Senapathy P 1987 RNA splice junctions of different classes of eukaryotes: sequence statistics and functional implications in gene expression. Nucleic Acids Res 15:7155–7174

Molecular Endocrinology **is published monthly by The Endocrine Society (http://www.endo-society.org), the foremost professional society serving the endocrine community.**